Author Manuscript

Author Manuscript

Author Manuscript

Author Manuscript

HHS Public Access

Author manuscript

J Neurosurg. Author manuscript; available in PMC 2016 February 09.

Published in final edited form as:

J Neurosurg. 2013 August ; 119(2): 427–433. doi:10.3171/2013.3.JNS122226.

Characterization of the blood-brain barrier of metastatic and primary malignant neoplasms:

Laboratory investigation

Edjah K. Nduom, M.D.[1,2], **Chunzhang Yang, Ph.D.**[1], **Marsha J. Merrill, Ph.D.**[1], **Zhengping Zhuang, M.D., Ph.D.**[1], and **Russell R. Lonser, M.D.**[1,3]

[1]Surgical Neurology Branch, National Institute of Neurological Disorders and Stroke, National Institutes of Health, Bethesda, Maryland [2]Department of Neurological Surgery, Emory University, Atlanta, Georgia [3]Department of Neurological Surgery, The Ohio State University, Columbus, Ohio

Abstract

Object—The astrocytic contribution to the blood-brain barrier (BBB) in metastatic and primary malignant brain tumors is not well understood. To better understand the vascular properties associated with metastatic and primary malignant brain tumors, the authors systematically analyzed the astrocytic component of the BBB in brain neoplasms.

Methods—Twelve patients who underwent resection of metastatic or primary brain neoplasms (4 metastatic lesions, 2 low-grade astrocytomas, 2 anaplastic astrocytomas, and 4 glioblastoma multiforme) were included. Clinical, MRI, operative, histopathological and immunohistochemical (glial fibrillary acidic protein [GFAP], CD31, and aquaporin 4 [AQ4]) findings were analyzed.

Results—Intratumoral regions of MRI enhancement corresponded with breakdown of the normal astrocyte–endothelial cell relationship in the BBB in metastatic deposits and malignant gliomas. Metastases demonstrated lack of perivascular GFAP and AQ4 on CD31-positive intratumoral vessels. At the metastasis-brain interface, normalization of GFAP and AQ4 staining associated with intraparenchymal vessels was observed. Intratumoral vasculature in enhancing regions of high-grade gliomas revealed gaps in GFAP and AQ4 staining consistent with disintegration of the normal astrocyte–endothelial cell association in the BBB. Intratumoral vasculature in low-grade and nonenhancing regions of high-grade gliomas maintained the normal astrocyte–endothelial cell relationship seen in an intact BBB, with GFAP- and AQ4-positive glial processes that were uniformly associated with the CD31-positive vasculature.

Conclusions—Regions of MRI enhancement in metastatic and primary malignancies correspond to areas of breakdown of the physiological astrocyte–endothelial cell relationship of

Address correspondence to: Russell R. Lonser, M.D., Department of Neurological Surgery, The Ohio State University Wexner Medical Center, 410 West 10th Avenue, N1047 Doan Hall, Columbus, Ohio 43210. russell.lonser@osumc.edu.

Author contributions to the study and manuscript preparation include the following. Conception and design: Lonser, Nduom, Yang, Zhuang. Acquisition of data: Nduom, Yang, Merrill. Analysis and interpretation of data: all authors. Drafting the article: Lonser, Nduom, Zhuang. Critically revising the article: all authors. Reviewed submitted version of manuscript: all authors. Approved the final version of the manuscript on behalf of all authors: Lonser. Administrative/ technical/material support: all authors. Study supervision: Lonser, Zhuang.

Author Manuscript Author Manuscript Author Manuscript Author Manuscript

the BBB, including loss of normal perivascular astrocytic architecture on GFAP and AQ4 immunohistochemistry. Nonenhancing areas are associated with preservation of the normal astrocyte–endothelial cell relationship of the intact BBB.

Keywords

blood-brain barrier; brain metastasis; brain tumor; contrast enhancement; glioma; oncology

The intact blood-brain barrier (BBB) prevents passage of larger hydrophilic molecules (> 180 Da) from the systemic vasculature into the CNS parenchyma.[14,24,27] The intact BBB is composed of tight junctions between vascular endothelial cells and is maintained by essential interactions between tightly apposed astrocytic foot processes and the vascular endothelial cells.[1,6,15,26,35,36] Magnetic resonance imaging contrast enhancement of cerebral metastases and malignant gliomas indicates that the BBB is compromised in certain CNS tumor types. Understanding the structural and cellular features of tumor-associated BBB disruption has implications for tumor vessel formation, potential therapeutic targets, and treatment strategies.

Data indicate that alterations in vascular endothelial cell tight junctions partially underlie neoplasm-associated BBB disruption.[11,19,31,37] Nevertheless, these changes do not explain many features of neoplastic BBB disruption, and further insight into the effects of the astrocytic contribution to the BBB in intracerebral neoplasia is needed. To gain deeper understanding into effects of the astrocytic contribution to the BBB in brain neoplasia, we systematically analyzed the vascular features of metastatic and primary brain tumors. Specifically, we examined the astrocyte–endothelial cell relationship of the BBB at sites of MRI contrast enhancement and compared it to the relationship at sites without contrast enhancement.

Methods

Patients and Tumors

Tumors were collected and analyzed under an institutional review board–approved protocol (NIH 03-N-0164). All patients provided informed consent for study participation.

Imaging Evaluation

Patients underwent high-resolution preoperative T1-weighted MRI before and after administration of a contrast agent. Lesions were classified as enhancing or nonenhancing based on the presence of hyperintensity on postcontrast T1-weighted MR images. T2-weighted sequences were used to assess for peritumoral edema, cyst formation, and tumor distribution (low-grade astrocytoma).

Tumor Specimen Collection

Resection of metastatic and primary tumors was performed with frameless stereotactic Instatrak 3000 (General Electric) or StealthStation Treon (Medtronic) guidance. Metastatic deposits were removed by en bloc resection that included removal of 2 mm of the immediately adjacent brain parenchyma surrounding the lesion. Low-grade gliomas were

Author Manuscript Author Manuscript Author Manuscript Author Manuscript

also removed by en bloc resection; upon removal, the tumor was marked to permit histoanatomical correlation with preoperative MRI. In patients undergoing resection of high-grade gliomas, biopsy specimens were obtained from enhancing and nonenhancing regions of the tumors and recorded to permit histological correlation with preoperative MRI. The remaining portion of the tumor was then removed en bloc and marked to permit histoanatomical correlation with preoperative MRI.

Histological Analysis

Histological examination of tissues stained with H & E was performed for diagnostic purposes and to define the morphological features of the tumor vasculature throughout the lesions and associated tumor-brain interface (when present). The MIB-1 proliferation index was determined for all tumors, and glial tumors were evaluated for GFAP expression. Pathological samples were submitted with detailed descriptions, including corresponding imaging findings.

Immunohistochemical Analysis

To assess perivascular astrocytic foot processes, double immunofluorescence staining for CD31 and GFAP was performed on sections from each tumor (rabbit anti-CD31 [EP3095, Millipore; 1:200] and mouse anti-GFAP [G3893, Sigma-Aldrich; 1:200]). We also evaluated astrocytic foot processes using AQ4, which is preferentially located within the basement membrane of these astrocytic processes. Double immunofluorescence staining for CD31 and AQ4 was performed on each tumor (mouse anti-CD31 [M0823, Dako; 1:200] and rabbit anti-AQ4 [AB2218, Millipore 1:200]). Secondary goat anti–rabbit IgG antibody absorbing at a wavelength of 594 nm (A21207, Invitrogen; 1:200) and goat anti–mouse IgG antibody at a wavelength of 488 nm (A21202, Invitrogen; 1:200) were applied to tissue samples. Vectashield HardSet mounting medium with 4′, 6-diamidino-2-phenylindole (DAPI) (Vector Laboratories) was used to create blue immunofluorescence at an excitation wavelength of 360 nm at sites containing DNA. Immunofluorescent images were captured using a Leica LSM 510 confocal microscope, while bright-field microscope images were captured using a Leica DM LB microscope with a Spot Imaging camera and software.

Results

Patient Characteristics

Twelve patients harboring 12 metastatic deposits or gliomas were included in the study (3 women, 9 men). Their mean age was 49.9 ± 15.8 years (range 23–74 years). A summary of their demographic and clinical characteristics is provided in Table 1.

Imaging Characteristics

Metastases—All metastatic deposits enhanced vividly and homogeneously on postcontrast T1-weighted MR images (Fig. 1). Metastatic deposits were found in the parietal, frontoparietal, and temporal lobes of the brain at the gray-white junction (Table 2). T2-weighted MRI demonstrated peritumoral edema that uniformly surrounded the deposits and extended into the immediately surrounding white matter.

Author Manuscript Author Manuscript Author Manuscript Author Manuscript

Low-Grade Gliomas—In each of the 2 patients with low-grade gliomas, the lesion was in the frontal lobe and was identified as a hypointense area on T1-weighted MRI that corresponded to a T2 hyperintensity in the same region (Fig. 2). There was no significant peritumoral edema and there was minimal mass effect on the immediately surrounding tissues. There was lack of contrast-enhancement on T1-weighted MRI in both cases of low-grade glioma.

Malignant Gliomas (Anaplastic Astrocytoma and Glioblastoma Multiforme)—All malignant gliomas demonstrated irregular enhancement on T1-weighted MRI except for 1 anaplastic astrocytoma that did not demonstrate evidence of contrast enhancement. Associated cerebral edema emanated from the tumors into the surrounding white matter and was associated with corresponding mass effect (Figs. 3–5).

Tumor Characteristics

Metastases—Metastatic deposits were histologically discrete lesions that demonstrated morphology consistent with the known primary tumor. A thin rim of GFAP-positive parenchyma surrounded the lesions. There was a distinct border between the neoplastic tissue and the surrounding brain (Fig. 1) that made analysis of the vasculature at the metastasis-brain interface possible.

Low-Grade Gliomas—Low-grade gliomas demonstrated increased cellularity within the cerebral white matter, consisting of GFAP-positive neoplastic cells. The neoplastic cells demonstrated evidence of cellular atypia. There was lack of increased mitotic activity, vascular proliferation, or pseudopalisading necrosis (Fig. 2).

Malignant Gliomas—Anaplastic astrocytomas demonstrated GFAP-positive cells, prominent mitoses, increased cellularity, and mitoses without vascular proliferation or necrosis. Glioblastoma multiforme specimens demonstrated GFAP-positive cells, prominent mitoses, increased cellularity, and mitoses with pseudopalisading necrosis (Figs. 3 and 5).

Correlation of Imaging and Astrocyte–Endothelial Cell Relationship

Metastases—Within metastatic deposits and consistent with disruption of the astrocytic component of the BBB, there was absence of GFAP or AQ4 immunoreactivity adjacent to CD31-positive vessels (Fig. 1). CD31-positive endothelial cells within the tumor mass were thin and dysmorphic (compared with normal parenchyma endothelial cells). Glial processes were absent within the metastases. The physiological astrocyte–endothelial cell relationship of the BBB was reconstituted at the tumor-brain interface surrounding metastases as demonstrated by tight orientation of the astrocytic foot processes and uniform AQ4 staining along the luminal side of the glial process surrounding each vessel.

Low-Grade Astrocytomas—The histological morphology of the intratumoral vasculature in low-grade gliomas was normal (Fig. 2). Vessels within the tumor tissues in low-grade astrocytomas were associated with tight circumferential orientation of GFAP-positive glial processes around the vasculature (Fig. 2). AQ4 staining was particularly intense and uniform along the luminal side of the glial processes surrounding each vessel.

Author Manuscript Author Manuscript Author Manuscript Author Manuscript

There was AQ4 and GFAP staining in the glioma cells, but these cells were relatively small in number as compared with the normal cells with typical glial processes.

High-Grade Gliomas—Consistent with breakdown of the astrocytic contribution to the BBB, gaps in GFAP or AQ4 immunoreactivity surrounding the vessels (Figs. 3, 4, and 5) in enhancing portions of high-grade gliomas were found. Diffuse GFAP and AQ4 staining was seen throughout enhancing lesions, showing disorganized glial staining that was associated with glioma cells. These cells did not have the normal elongated processes expected of typical glial cells, but rather were discrete, atypical cells without organized glial processes. There was an absence of immunofluorescence of GFAP or AQ4 surrounding the vasculature of these lesions. Nonenhancing regions were associated with return of the tight orientation of the glial processes, and uniform AQ4 staining was found along the luminal side of the glial process surrounding the CD31-positive vasculature.

Discussion

Previous Studies

The normal BBB in brain has been well characterized and includes tight junctions between vascular endothelial cells as well as essential interactions between immediately surrounding astrocyte processes and endothelial cells.[1,6,28] Previous studies have examined histological and immunohistochemical features of tight junctions associated with vascular endothelial cells of metastatic and primary tumors. Alterations in claudin expression at tight junctions have been demonstrated in tumors, as well as inflammatory disorders of the nervous system,[19,31,37] suggesting that the tight junctions are disrupted and are associated, at least in part, with BBB breakdown in a variety of CNS pathological states, including neoplasia.

While changes in tight junction morphology and function have been implicated with BBB breakdown in tumor vasculature, the potential changes associated with the astrocytic component of the BBB have not been defined. Better understanding of astrocyte–endothelial cell interactions in the BBB of brain tumors can provide insight into mechanisms linked with neoplasia-associated BBB breakdown and tumor vascular development and may present opportunities for targeted treatment of tumor vasculature. Moreover, better understanding of the astrocyte–endothelial cell relationship in disease states can provide critical understanding to improve therapy in conditions associated with BBB breakdown. Here, we characterized the astrocytic contribution to the BBB in brain tumors.

Current Study Analysis

To best evaluate the integrity of the astrocytic component of the BBB in a variety of neoplastic states, we performed immunohistochemical analysis on metastatic and primary (low- and high-grade glioma) brain tumors. CD31, or platelet endothelial cell adhesion molecule, is a well-established and well-characterized marker of vessels.[2] To define astrocyte interactions on tumor vessels, we used GFAP (intracellular glial filaments)[28] to demonstrate astrocytic distribution and morphology. Aquaporin 4 immunohistochemistry was used to demonstrate the integrity (or lack thereof) of glial basement membrane surrounding blood vessels.[34] For comparison purposes, the intact BBB demonstrates CD31-

Author Manuscript Author Manuscript Author Manuscript Author Manuscript

positive vessels tightly surrounded by GFAP-positive glial processes with AQ4 staining lining the luminal side of the glial processes, consistent with a phenotypically normal basement membrane.[9]

Metastases—Breakdown of the BBB in metastatic deposits is clearly demonstrated by discrete uniform intralesional gadolinium-based contrast enhancement on MRI. Consistent with these imaging findings, previous studies have indicated that endothelial cell tight junctions within brain metastases are abnormal and disrupted.[10] Further, the current study demonstrates that the astrocytic contribution to the BBB throughout the metastatic deposits is also disrupted. Consequently, BBB barrier disruption in metastatic deposits appears to be the result of both tight junction dysfunction and breakdown of normal astrocyte– endothelial cell interaction. Alternatively, near the periphery of the metastatic deposits (the metastasis-brain interface), vessels reconstituted a normal astrocyte–endothelial cell relationship with tight association of the glial processes surrounding vessels.

Glioma—Low-grade gliomas demonstrated a tight arrangement of astrocytic processes and intact astrocytic basement membrane surrounding intratumoral vessels that is consistent with an intact astrocytic component of the BBB. Based on the normal appearance of intratumoral vessels in these tumors, it does not appear that significant angiogenesis occurs in these lesions. Consistent with known glioma cell biology it seems plausible that neoplastic cells invade normal brain and receive nutrients by diffusion from existing phenotypically normal astrocyte– endothelial cell interactions.[7] Although there is increased neoplastic cellularity in these lesions, unaffected astrocytes formed tight processes that surround vessels and a basement membrane that produced a phenotypically normal BBB. The presence of a normal astrocyte–endothelial cell relationship within these nonenhancing tumors was consistent with MRI evidence of an intact BBB.

Consistent with breakdown of the BBB in high-grade gliomas, MRI enhancement was found in portions of these lesions. Regions of MRI enhancement in high-grade gliomas demonstrated loss of the normal tight astrocytic fibrillary arrangement of glial processes and associated basement membrane surrounding the intratumoral vasculature. There was diffuse GFAP and AQ4 staining throughout the tumor but a lack of the normal uniform GFAP and AQ4 staining pattern association with an intact BBB. Specifically, there were gaps in GFAP and AQ4 staining between vessels and surrounding glial processes consistent with breakdown of the astrocytic component of the BBB. The immunohistochemistry-imaging correlation revealed a consistent association between BBB breakdown demonstrated by contrast-enhanced MRI and disruption of the astrocyte–endothelial cell relationship.

Clinical Implications

The data from the current study can provide insight into BBB breakdown and peritumoral edema formation. Specifically, the breakdown of the BBB in metastases and high-grade gliomas is associated with disruption of endothelial tight junctions. Extravasation of plasma ultrafiltrate through leaky endothelial vessels underlies peritumoral edema formation.[20–22] Dexamethasone reduces BBB permeability at endothelial tight junctions and can reduce

Author Manuscript Author Manuscript Author Manuscript Author Manuscript

peritumoral edema.[8,12,16,18] These steroid effects on the BBB appear to replicate the properties of the perivascular astrocytes in the brain.[3,4,29,33]

Conclusions

It is critical to understand the impact of nervous system neoplasia on the BBB. Not only do the current findings provide insight into the effect of BBB breakdown on peritumoral edema, but they also provide a deeper understanding of tumor development, progression, and treatment.[25] Specifically, understanding the alterations in the astrocyte relationship to the vascular endothelial cells in the BBB permits deeper comprehension of mechanisms associated with metastasis development,[17] chemoresistance in metastatic and primary tumors,[13,32] mechanisms to improve drug delivery,[5,23] and immune cell trafficking in neoplasia.[30]

Acknowledgments

Disclosure

This work was supported by the intramural program of the National Institute of Neurological Disorders and Stroke at the National Institutes of Health.

Abbreviations used in this paper

AQ4	aquaporin 4
BBB	blood-brain barrier
GFAP	glial fibrillary acidic protein

References

1. Abbott NJ, Rönnbäck L, Hansson E. Astrocyte-endothelial interactions at the blood-brain barrier. Nat Rev Neurosci. 2006; 7:41–53. [PubMed: 16371949]
2. Albelda SM, Muller WA, Buck CA, Newman PJ. Molecular and cellular properties of PECAM-1 (endoCAM/CD31): a novel vascular cell-cell adhesion molecule. J Cell Biol. 1991; 114:1059–1068. [PubMed: 1874786]
3. Antonetti DA, Barber AJ, Hollinger LA, Wolpert EB, Gardner TW. Vascular endothelial growth factor induces rapid phosphorylation of tight junction proteins occludin and zonula occluden 1. A potential mechanism for vascular permeability in diabetic retinopathy and tumors. J Biol Chem. 1999; 274:23463–23467. [PubMed: 10438525]
4. Antonetti DA, Barber AJ, Khin S, Lieth E, Tarbell JM, Gardner TW. Vascular permeability in experimental diabetes is associated with reduced endothelial occludin content: vascular endothelial growth factor decreases occludin in retinal endothelial cells. Diabetes. 1998; 47:1953–1959. [PubMed: 9836530]
5. Caraglia M, De Rosa G, Salzano G, Santini D, Lamberti M, Sperlongano P, et al. Nanotech revolution for the anti-cancer drug delivery through blood-brain barrier. Curr Cancer Drug Targets. 2012; 12:186–196. [PubMed: 22268384]
6. Cardoso FL, Brites D, Brito MA. Looking at the blood-brain barrier: molecular anatomy and possible investigation approaches. Brain Res Brain Res Rev. 2010; 64:328–363.
7. Claes A, Idema AJ, Wesseling P. Diffuse glioma growth: a guerilla war. Acta Neuropathol. 2007; 114:443–458. [PubMed: 17805551]

Author Manuscript Author Manuscript Author Manuscript Author Manuscript

8. Ellemann K, Christensen L, Gjerris F, Briand P, Kruse-Larsen C. Glucocorticoid receptors in glioblastoma multiforme: a new approach to antineoplastic glucocorticoid therapy. Acta Neurochir (Wien). 1988; 93:6–9. [PubMed: 2843007]
9. Ezan P, André P, Cisternino S, Saubaméa B, Boulay AC, Doutremer S, et al. Deletion of astroglial connexins weakens the blood-brain barrier. J Cereb Blood Flow Metab. 2012; 32:1457–1467. [PubMed: 22472609]
10. Fazakas C, Wilhelm I, Nagyoszi P, Farkas AE, Haskó J, Molnár J, et al. Transmigration of melanoma cells through the blood-brain barrier: role of endothelial tight junctions and melanoma-released serine proteases. PLoS ONE. 2011; 6:e20758. [PubMed: 21674054]
11. Fidler IJ, Yano S, Zhang RD, Fujimaki T, Bucana CD. The seed and soil hypothesis: vascularisation and brain metastases. Lancet Oncol. 2002; 3:53–57. [PubMed: 11905606]
12. Förster C, Waschke J, Burek M, Leers J, Drenckhahn D. Glucocorticoid effects on mouse microvascular endothelial barrier permeability are brain specific. J Physiol. 2006; 573:413–425. [PubMed: 16543270]
13. Fortin D. The blood-brain barrier: its influence in the treatment of brain tumors metastases. Curr Cancer Drug Targets. 2012; 12:247–259. [PubMed: 22229251]
14. Habgood MD, Begley DJ, Abbott NJ. Determinants of passive drug entry into the central nervous system. Cell Mol Neurobiol. 2000; 20:231–253. [PubMed: 10696512]
15. Hawkins BT, Davis TP. The blood-brain barrier/neurovascular unit in health and disease. Pharmacol Rev. 2005; 57:173–185. [PubMed: 15914466]
16. Heiss JD, Papavassiliou E, Merrill MJ, Nieman L, Knightly JJ, Walbridge S, et al. Mechanism of dexamethasone suppression of brain tumor-associated vascular permeability in rats. Involvement of the glucocorticoid receptor and vascular permeability factor. J Clin Invest. 1996; 98:1400–1408. [PubMed: 8823305]
17. Kienast Y, von Baumgarten L, Fuhrmann M, Klinkert WE, Goldbrunner R, Herms J, et al. Real-time imaging reveals the single steps of brain metastasis formation. Nat Med. 2010; 16:116–122. [PubMed: 20023634]
18. Kotsarini C, Griffiths PD, Wilkinson ID, Hoggard N. A systematic review of the literature on the effects of dexamethasone on the brain from in vivo human-based studies: implications for physiological brain imaging of patients with intracranial tumors. Neurosurgery. 2010; 67:1799–1815. [PubMed: 21107211]
19. Liebner S, Fischmann A, Rascher G, Duffner F, Grote EH, Kalbacher H, et al. Claudin-1 and claudin-5 expression and tight junction morphology are altered in blood vessels of human glioblastoma multiforme. Acta Neuropathol. 2000; 100:323–331. [PubMed: 10965803]
20. Lohle PN, Wurzer HA, Seelen PJ, Kingma LM, Go KG. Analysis of fluid in cysts accompanying various primary and metastatic brain tumours: proteins, lactate and pH. Acta Neurochir (Wien). 1998; 140:14–19. [PubMed: 9522902]
21. Lohle PN, Wurzer HA, Seelen PJ, Kingma LM, Go KG. The pathogenesis of cysts accompanying intra-axial primary and metastatic tumors of the central nervous system. J Neurooncol. 1998; 40:277–285. [PubMed: 10066101]
22. Lonser RR, Vortmeyer AO, Butman JA, Glasker S, Finn MA, Ammerman JM, et al. Edema is a precursor to central nervous system peritumoral cyst formation. Ann Neurol. 2005; 58:392–399. [PubMed: 16130092]
23. Mehta AI, Brufsky AM, Sampson JH. Therapeutic approaches for HER2-positive brain metastases: circumventing the blood-brain barrier. Cancer Treat Rev. 2013; 39:261–269. [PubMed: 22727691]
24. Mitic LL, Anderson JM. Molecular architecture of tight junctions. Annu Rev Physiol. 1998; 60:121–142. [PubMed: 9558457]
25. Muldoon LL, Alvarez JI, Begley DJ, Boado RJ, Del Zoppo GJ, Doolittle ND, et al. Immunologic privilege in the central nervous system and the blood-brain barrier. J Cereb Blood Flow Metab. 2013; 33:13–21. [PubMed: 23072749]
26. Persidsky Y, Ramirez SH, Haorah J, Kanmogne GD. Blood-brain barrier: structural components and function under physiologic and pathologic conditions. J Neuroimmune Pharmacol. 2006; 1:223–236. [PubMed: 18040800]

Author Manuscript Author Manuscript Author Manuscript Author Manuscript

27. Petty MA, Lo EH. Junctional complexes of the blood-brain barrier: permeability changes in neuroinflammation. Prog Neurobiol. 2002; 68:311–323. [PubMed: 12531232]
28. Raff MC, Fields KL, Hakomori SI, Mirsky R, Pruss RM, Winter J. Cell-type-specific markers for distinguishing and studying neurons and the major classes of glial cells in culture. Brain Res. 1979; 174:283–308. [PubMed: 385109]
29. Romero IA, Radewicz K, Jubin E, Michel CC, Greenwood J, Couraud PO, et al. Changes in cytoskeletal and tight junctional proteins correlate with decreased permeability induced by dexamethasone in cultured rat brain endothelial cells. Neurosci Lett. 2003; 344:112–116. [PubMed: 12782340]
30. Rössler K, Neuchrist C, Kitz K, Scheiner O, Kraft D, Lassmann H. Expression of leucocyte adhesion molecules at the human blood-brain barrier (BBB). J Neurosci Res. 1992; 31:365–374. [PubMed: 1374132]
31. Seelbach M, Chen L, Powell A, Choi YJ, Zhang B, Hennig B, et al. Polychlorinated biphenyls disrupt blood-brain barrier integrity and promote brain metastasis formation. Environ Health Perspect. 2010; 118:479–484. [PubMed: 20064788]
32. Spiegl-Kreinecker S, Buchroithner J, Elbling L, Steiner E, Wurm G, Bodenteich A, et al. Expression and functional activity of the ABC-transporter proteins P-glycoprotein and multidrug-resistance protein 1 in human brain tumor cells and astrocytes. J Neurooncol. 2002; 57:27–36. [PubMed: 12125964]
33. Underwood JL, Murphy CG, Chen J, Franse-Carman L, Wood I, Epstein DL, et al. Glucocorticoids regulate transendothelial fluid flow resistance and formation of intercellular junctions. Am J Physiol. 1999; 277:C330–C342. [PubMed: 10444410]
34. Warth A, Kröger S, Wolburg H. Redistribution of aquaporin-4 in human glioblastoma correlates with loss of agrin immunoreactivity from brain capillary basal laminae. Acta Neuropathol. 2004; 107:311–318. [PubMed: 14735305]
35. Willis CL, Leach L, Clarke GJ, Nolan CC, Ray DE. Reversible disruption of tight junction complexes in the rat blood-brain barrier, following transitory focal astrocyte loss. Glia. 2004; 48:1–13. [PubMed: 15326610]
36. Willis CL, Nolan CC, Reith SN, Lister T, Prior MJ, Guerin CJ, et al. Focal astrocyte loss is followed by microvascular damage, with subsequent repair of the blood-brain barrier in the apparent absence of direct astrocytic contact. Glia. 2004; 45:325–337. [PubMed: 14966864]
37. Wolburg H, Wolburg-Buchholz K, Kraus J, Rascher-Eggstein G, Liebner S, Hamm S, et al. Localization of claudin-3 in tight junctions of the blood-brain barrier is selectively lost during experimental autoimmune encephalomyelitis and human glioblastoma multiforme. Acta Neuropathol. 2003; 105:586–592. [PubMed: 12734665]

Author Manuscript Author Manuscript Author Manuscript Author Manuscript

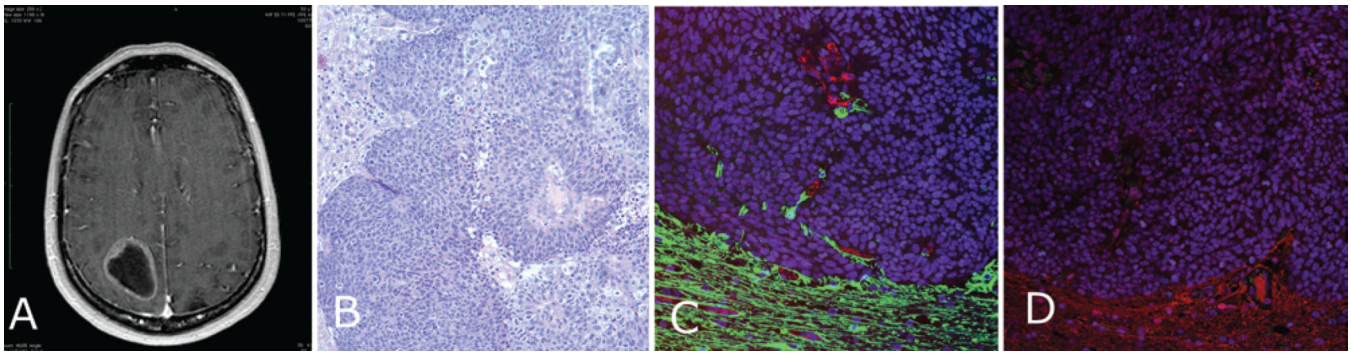

Fig. 1. Metastatic cervical carcinoma (Case 9)

A: Contrast-enhanced T1-weighted MR image showing a ring-enhancing metastatic parietooccipital lesion. **B**: Photomicrograph of an H & E–stained specimen showing metastatic cervical carcinoma invading the surrounding brain. **C**: Immunostained specimen demonstrating the border between tumor cells negative for GFAP *(green)* expression and the GFAP-positive surrounding brain. CD31 is shown with *red* immunofluorescence. The glial processes associated with the vessels at the periphery are evident on this micrograph. **D**: This panel shows a similar image with AQ4 immunofluorescence *(red)*, with the AQ4 showing a small indent into the tumor but being lost further inside the mass.

Author Manuscript Author Manuscript Author Manuscript Author Manuscript

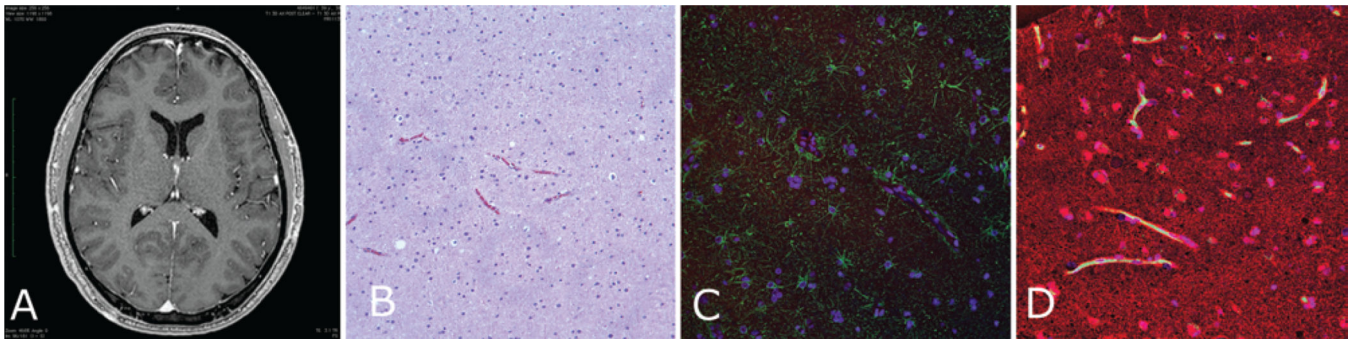

Fig. 2. Fibrillary astrocytoma (Case 7)

A: Preoperative contrast-enhanced T1-weighted MR image revealing a nonenhancing left frontal lesion, which is evident only as an asymmetrical hypointense mass lesion along the falx. **B**: An H & E–stained specimen showing a slightly hypercellular lesion. **C**: Specimen stained for GFAP *(green)* showing tight alignment of thin glial filaments surrounding the CD31-positive vasculature *(red)*. **D**: Specimen stained for AQ4 *(red)* similarly showing intense AQ4-positive staining around the *green* CD31-positive vessels.

Author Manuscript Author Manuscript Author Manuscript Author Manuscript

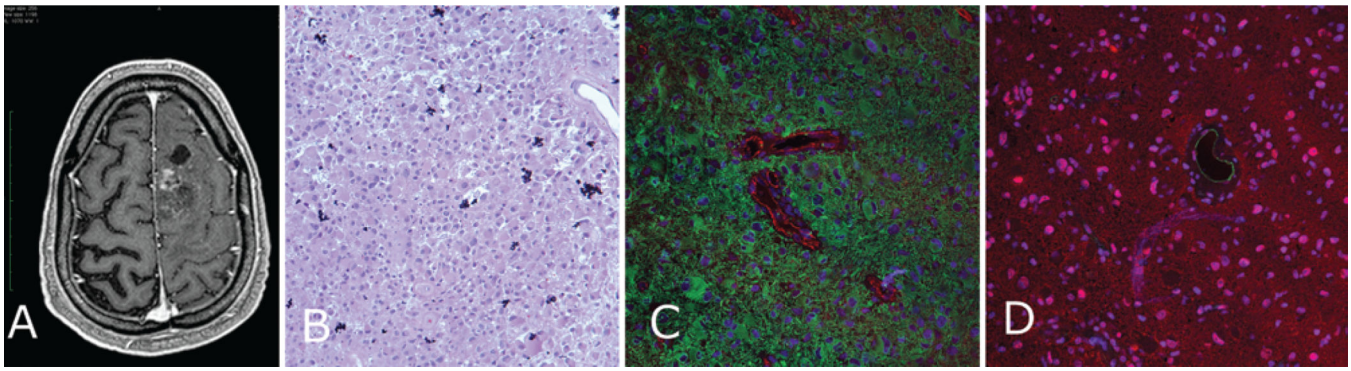

Fig. 3. Anaplastic astrocytoma (Case 3)

A: Preoperative T1-weighted MR image showing an enhancing Grade III glioma. **B**: An H & E–stained specimen showing a very hypercellular lesion. **C**: Immunostained specimen showing diffuse GFAP *(green)* staining with loss of the tight organization of GFAP filaments around the *red* CD31-positive vessels. **D**: Specimen stained for AQ4 *(red)* also showing diffuse staining with no strong border formed around the CD31-positive vessels *(green)*.

Author Manuscript Author Manuscript Author Manuscript Author Manuscript

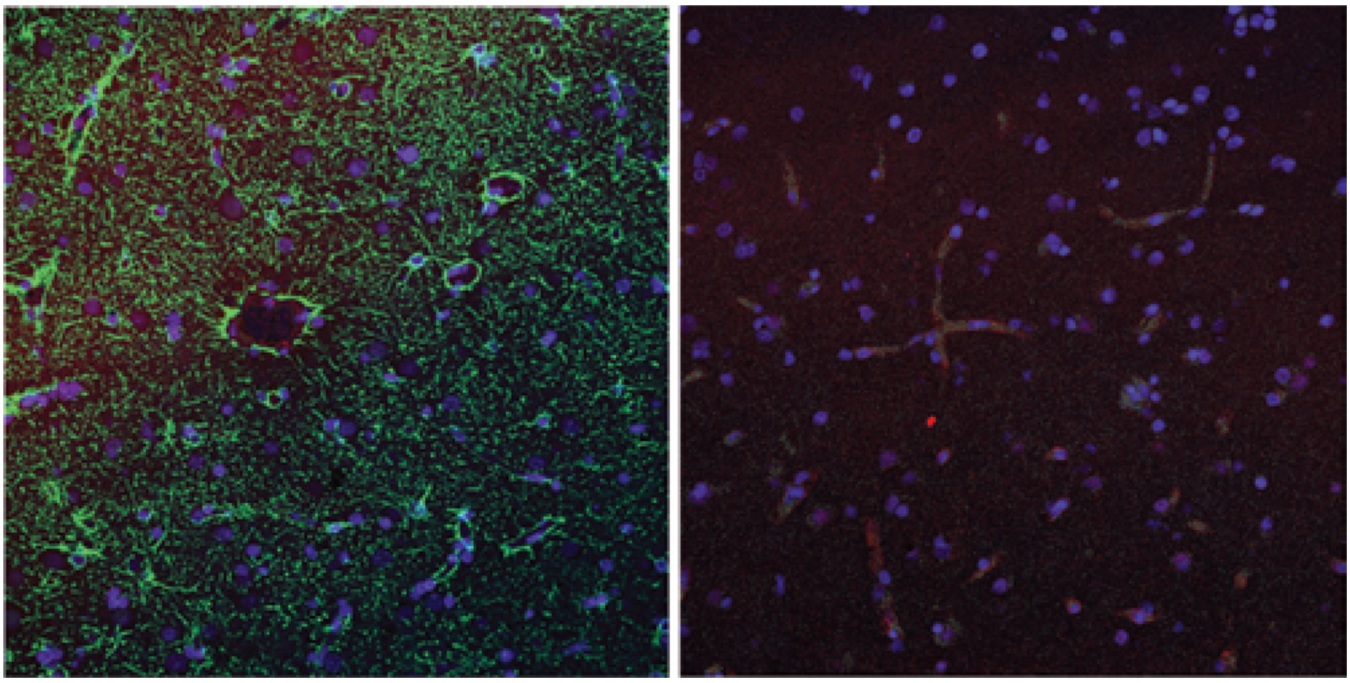

Fig. 4. Nonenhancing tissue

Left: Nonenhancing region of glioblastoma multiforme (Case 5). The *green* immunofluorescence represents GFAP staining, indicating glial processes which wrap tightly around the CD31-positive *(red)* vasculature. **Right:** Sample from nonenhancing brain tissue resected together with a metastasis (Case 9), with *red* immunofluorescence showing AQ4 staining tightly around the *green* CD31-positive vessels.

Author Manuscript Author Manuscript Author Manuscript Author Manuscript

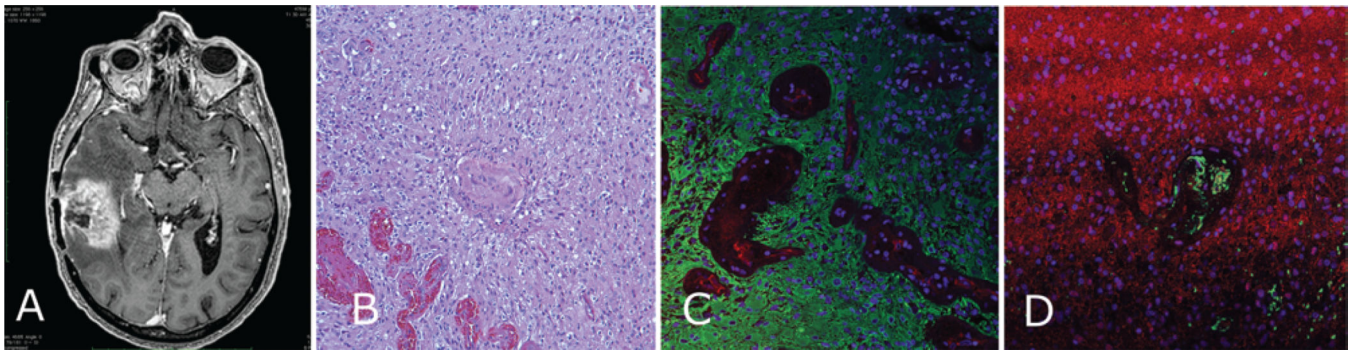

Fig. 5. Enhancing region of glioblastoma (Case 4)

A: Preoperative contrast-enhanced T1-weighted MR image showing enhancing right temporal lesion. **B**: Photomicrograph of resected tissue demonstrating glioblastoma with extreme hypercellularity and microvascular proliferation. **C**: Immunostained specimen showing complete loss of GFAP-positive *(green)* organization of glial processes, with diffuse immunostaining throughout the neoplastic cells of the tumor and no tight junctions around the vasculature (CD31, *red*). **D**: Specimen stained for AQ4 *(red)* demonstrating a lack of organization around the vasculature (CD31, *green*).

Author Manuscript

Author Manuscript

Author Manuscript

Author Manuscript

TABLE 1

Demographic and clinical characteristics

Case No.	Age (yrs), Sex	Pathology	Enhancement*
1	64, M	glioblastoma multiforme	yes
2	23, M	anaplastic astrocytoma	no
3	27, M	anaplastic astrocytoma	yes
4	74, M	glioblastoma multiforme	yes
5	67, F	glioblastoma multiforme	yes
6	62, M	metastatic melanoma	yes
7	39, M	low-grade astrocytoma	no
8	45, M	metastatic melanoma	yes
9	51, F	metastatic cervical cancer	yes
10	40, M	glioblastoma multiforme	yes
11	54, M	low-grade astrocytoma	no
12	53, F	metastatic adenocarcinoma	yes

*Contrast enhancement in tumors on MRI.

Author Manuscript

Author Manuscript

Author Manuscript

Author Manuscript

TABLE 2

Histological and immunohistochemical findings

		Vascular Immunohistochemical Features		
Tumor Type	**Vascular & Glial Morphology**	**CD31**	**GFAP**	**AQ4**
metastasis	thin-walled vessels, no astrocytes w/in lesion	positive staining of thin-walled vessel	no staining w/in bulk of lesion, but reconstitution of astrocytic processes at metastasis-brain interface	no staining w/in bulk of lesion, but reconstitution of normal basement membrane at metastasis-brain interface
low-grade glioma	normal-appearing vasculature (endothelial cells), astrocytes w/ normal elongated processes apposing each other & tightly associated w/ the vasculature w/in lesion	positive staining of normal-appearing vasculature w/in region of tumor	staining of astrocytic process tightly associated w/ vessels w/in scattered neoplastic cells w/ dysmorphic nuclei	intense staining surrounding vasculature throughout lesion
malignant glioma* enhancing region	scattered glomeruloid & thick-walled vessels, absence of normal astrocyte architecture	positive staining of thick-walled vasculature, including capillaries	diffuse staining, associated w/ neoplastic cells, no discernible elongated astrocytic processes, gaps in staining surrounding vasculature	diffuse AQ4 staining associated w/ neoplastic cells, gaps of AQ4 staining surrounding vasculature
nonenhancing region	normal-appearing cerebral vasculature, astrocytes w/ normal elongated processes apposing each other & tightly associated w/ vasculature w/in nonenhancing portions of lesion	positive staining of normal- appearing vasculature	staining of glial processes, tightly associated w/ vessels, together w/ scattered staining of neoplastic cells w/ dysmorphic nuclei	intense staining surrounding vasculature throughout lesion

*Enhancing region: contrast enhancement on MRI after intravenous contrast administration. Nonenhancing region: lack of contrast enhancement on MRI after intravenous contrast administration.